Mechanochemical synthesis of metallic Ag_2F and application to $Ag_3MoO_3F_3$ based nanocomposites for lithium batteries

Wei Tong[*], Glenn G. Amatucci

Energy Storage Research Group, Department of Materials Science and Engineering, Department of Biomedical Engineering, Rutgers, The State University of New Jersey, North Brunswick, NJ 08902, United States

ABSTRACT

Metallic Ag_2F phase has been successfully synthesized through the mechanochemical reaction of Ag and AgF. Its unique metallic character leads to a good electronic conductivity of 7.89×10^{-2} S cm^{-1}. The efficacy of silver molybdenum oxyfluoride (SMOF) composites consisting of various conducting matrices (carbon black, Ag_2F and Ag) for lithium battery was investigated through discharge rate studies. Results indicate that Ag_2F phase can be utilized as an alternative conductive additive with a high density.

© 2010 Elsevier B.V. All rights reserved.

1. Introduction

Over the past decade, extensive efforts have been made to search for new cathode materials of higher energy and good power for lithium battery energy storage technology [1–4]. One such need is driven by the development of implantable biomedical devices such as cardiac defibrillators [5,6]. However, these two performance factors are difficult to accomplish concurrently because of the losses in capacity when the batteries are cycled at a high current density [7]. Among a number of factors affecting the power density in the battery, the most critical one besides the choice of the electrolyte is the fast Li^+ and e^- transport in the electrode materials [8,9]. In light of these requirements, electrode materials with high intrinsic electronic conductivities or the use of such materials within composites of electronically conductive additives which are volumetrically efficient are worthwhile pursuits.

Presently, the widely used battery is $Li–I_2$ system for lower rate applications such as the pacemaker. The higher rate applications such as the cardiac defibrillator are powered by silver vanadium oxide or its oxyfluoride derivatives [10–13]. However, efforts are still being made for the search of new materials with better performance. Recently, we have reported new nanocompounds, silver metal oxyfluoride perovskites of the proposed formula $Ag^{1+}_3M^{n+}(O_zF_{6-z})$ (M = Mo, $n = 6$; M = Nb, $n = 5$) [14–18]. Relative to

pure silver fluorides, these new compounds exhibited appreciable mixed conductivity as evidenced by their good reaction kinetics. Preliminary studies indicated that these compounds can deliver higher energy density than that of silver vanadium oxide, state of the art, at the desired output voltage >3 V. However, the rate capability of these compounds still needs to be further improved. We have shown the overall electrochemical performance of silver metal oxyfluorides could be improved through the use of conductive carbon. However, the addition of conductive carbon would significantly decrease the volumetric energy density due to its very low density. Therefore, it would be ideal to find an alternative conductive additive, which would be able to enhance the electronic conductivity without affecting the overall volumetric energy density.

Ag_2F has anti-CdI_2 structure consisting of hexagonal closed-packed layers of Ag and F atoms (Fig. 1) [19–22]. This structure essentially consists of repeating layers of AgF and Ag. Its structure is directly responsible for Ag_2F being one of the few metallic conducting fluorides. This phase has been previously prepared by the electrolytical method [21]. In our earlier work, metallic Ag_2F secondary phase was observed to form in situ during the formation of silver molybdenum oxyfluoride (SMOF) with Ag:Mo ≥ 4. The presence of Ag_2F was believed to be responsible for the good electrochemical performance found in the SMOF sample of Ag:Mo = 5.67 [22]. As such, it generated our interest to utilize Ag_2F phase as the conductive agent due to its unique metallic character within Ag layers and its high density (8.76 g cc^{-1}). In this paper, we focus our attention on the synthesis of pure Ag_2F phase through a facile mechanochemical reaction. The effects of metallic Ag_2F

* Corresponding author. Tel.: +1 732 932 6850; fax: +1 732 932 6855.
E-mail addresses: weitong@eden.rutgers.edu, wtongru@gmail.com (W. Tong).
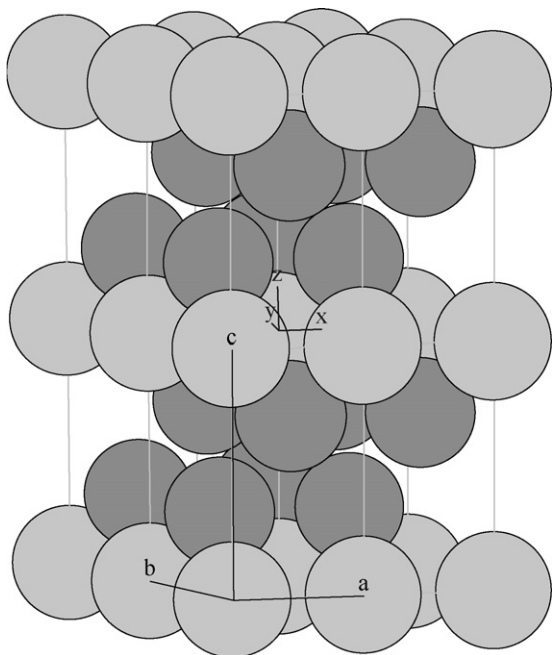
Fig. 1. The crystal structure of Ag_2F. Dark grey circle is Ag and light grey circle is F.

phase on the rate capabilities of SMOF perovskite are investigated in detail.

2. Experimental

2.1. Materials fabrication

The metallic Ag_2F phase was prepared by high-energy milling 1 g of the pre-ground stoichiometric precursors of Ag and AgF (Aldrich, 99%) for the designated time in a Spex 8000 mill. Both the high-energy milling cell and milling media are made of hardened steel. All the assemblies were performed inside a He-filled glove box at $-80\,°C$ dew point, therefore minimizing the contamination from moisture or oxygen. In this study, silver molybdenum oxyfluoride (SMOF) perovskite, to investigate the conductivity effect of the metallic Ag_2F phase, was fabricated by high-energy milling 70 mol% AgF:30 mol% MoO_3 for 45 min. XRD analysis indicated the resulting phase was almost pure SMOF with a very small amount of Ag secondary phase.

2.2. Physical characterization (X-ray powder diffraction)

X-ray powder diffraction (XRD) analyses were performed on a Scintage X2 diffractometer using Cu Kα radiation. XRD data were collected at $0.6°\,min^{-1}$ in the 2θ range of 15–80°. The samples to be analyzed were placed on the glass slides, covered by Kapton film and sealed by a layer of vacuum grease around the perimeter to minimize air exposure.

2.3. Electrochemical characterization

The effect of the metallic Ag_2F phase on the rate capability of SMOF ($x = 70$) was investigated by several series of electrochemical studies in 2032 coin cells (Hohsen Corp.) in the form of: (1) pure SMOF powder, (2) manually mixed composite of 80 wt% SMOF:20 wt% carbon black (Super P, MMM), (3) manually mixed 70 SMOF:30 Ag_2F (wt%), (4) high-energy milled (20 min) 70 SMOF:30 Ag_2F (wt%), (5) high-energy milled (45 min) mixtures of AgF, MoO_3 and Ag precursors with the intended stoichiometry of 70 SMOF

to 30 Ag_2F (wt%). The powder electrodes were tested electrochemically vs. lithium (Johnson Matthey), which were physically separated by a layer of Celgard separator and Whatman GF/D glass fiber separators saturated in 1 M $LiPF_6$ in ethylene carbonate: dimethyl carbonate (EC:DMC, 1:1 by volume) (Ferro). All the cells were assembled in a He-filled glove box and controlled by a MacPile galvanostat cycler (Biologic, Claix, France). Cells were cycled between 4 and 2 V at $22\,°C$ under a designated current, namely, 7.58, 20, 30, 60, 120 mA g^{-1}.

3. Results

3.1. Physical characterization

The metallic Ag_2F phase was initially fabricated by high-energy milling 50 mol% Ag and 50 mol% AgF for 45 min based on the stoichiometry: $Ag + AgF \rightarrow Ag_2F$. To further purify the Ag_2F composition, synthesis parameters were investigated including the initial Ag and AgF stoichiometry and high-energy milling time. The evolution of the Ag_2F phase formed by high-energy milling process has been examined by XRD. It can be clearly seen in Fig. 2 that Ag_2F phase was fully developed at the composition of 40 mol% Ag, however, small residual peaks related to AgF are present. Increasing the Ag content to 50 mol% resulted in the formation of the Ag_2F major phase along with a small quantity of both AgF and Ag residual phases. A further increase of Ag composition to 60 mol% resulted in the disappearance of any AgF residual phase and the increase of Ag residuals. To investigate the impact of milling time, 40 mol% Ag and 60 mol% AgF were mechanically milled for 90 min rather than 45 min. As revealed by XRD, this synthesis procedure resulted in the production of phase pure Ag_2F. The initial refinement and resulting indexing (Table 1) of the XRD pattern of the Ag_2F phase was performed on this relatively pure sample. The refined lattice parameters of $a = b = 3.000 \pm 0.000$ Å, $c = 5.698 \pm 0.001$ Å, $\alpha = \beta = 90°$, $\gamma = 120°$ agree well with the lattice parameters of $a = b = 3.0016$ Å, $c = 5.7014$ Å, $\alpha = \beta = 90°$, $\gamma = 120°$ as identified for Ag_2F in powder diffraction file # 00-17-0325. This confirmed the as-fabricated Ag_2F phase is of a hexagonal structure. As shown in Fig. 3, close examination of the observed XRD pattern shows the Bragg peaks with the indexing (0 0 L) along c-axis direction have an exceptionally
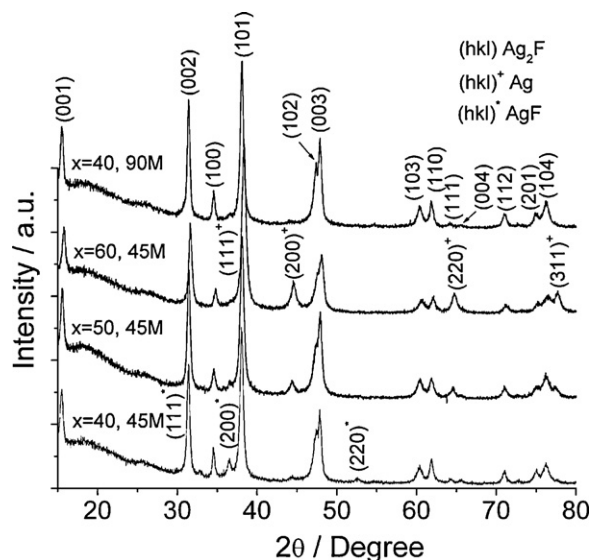

Fig. 2. XRD pattern of high-energy milled xAg:$(1 − x)$ AgF (mol%) for a designated time. Label x and M indicate Ag content (mol%) in the precursor powder and high-energy milling time, respectively.

Table 1
Observed d-spacing and indexing of the as-fabricated Ag_2F phase based on a hexagonal unit cell.

$h\,k\,l$	d_{obs} (Å)	d_{calc} (Å)	$d_{obs} - d_{calc}$
0 0 1	5.702	5.698	5×10^{-3}
0 0 2	2.850	2.849	1×10^{-3}
1 0 0	2.596	2.598	-2×10^{-3}
1 0 1	2.363	2.364	-1×10^{-3}
1 0 2	1.921	1.920	1×10^{-3}
0 0 3	1.899	1.899	0
1 0 3	1.533	1.533	0
1 1 0	1.500	1.500	0
1 1 2	1.327	1.327	0
2 0 1	1.267	1.267	0
1 0 4	1.249	1.249	0

$a = b = 3.000 \pm 0.000$ (Å), $c = 5.698 \pm 0.001$ (Å), $\alpha = \beta = 90°$, $\gamma = 120°$, $V = 44.41$ (Å^3).

strong intensity, indicating the Ag_2F phase exhibited some degree of preferred orientation.

3.2. Electrochemical characterization

Pure SMOF: Based on the formula, the theoretical capacity of $Ag_3MoO_3F_3$ is calculated to be 153 mAh g^{-1} associated to a 3 electron silver displacement/reduction at the voltage >3 V and a 2 electron reduction of Mo^{6+} to Mo^{4+} at the voltage <3 V resulting in a total capacity of 255 mAh g^{-1}. Preliminary electrochemical characterization indicated that close to theoretical capacity was achieved when discharging a SMOF electrode containing 12 wt% carbon black to 1.5 V along with three plateaus around 3.6, 3.1 and 2.1 V [15]. The reaction mechanism of SMOF was investigated by in situ XRD, Raman and XAS. The first two lithium insertion at approximately 3.6 V is consistent with the reduction of two Ag^+ to Ag^0, the third lithium insertion at a lower voltage of 3.1 V is related to the reduction of the third Ag^+ to Ag^0 and the final two lithium insertion around a plateau of 2.1 V is associated to a theoretical reduction of Mo^{6+} to Mo^{4+} [23].

As a benchmark, the rate capability of the pure SMOF perovskite powder without any conductive additive was evaluated to a peak current of 120 mA g^{-1}. In this paper, the 2 V plateaus related to $Mo^{6+} \rightarrow Mo^{4+}$ (<2.25 V) are not shown in the voltage profiles of the SMOF primary cells. As shown in Fig. 4, SMOF exhibited respectable

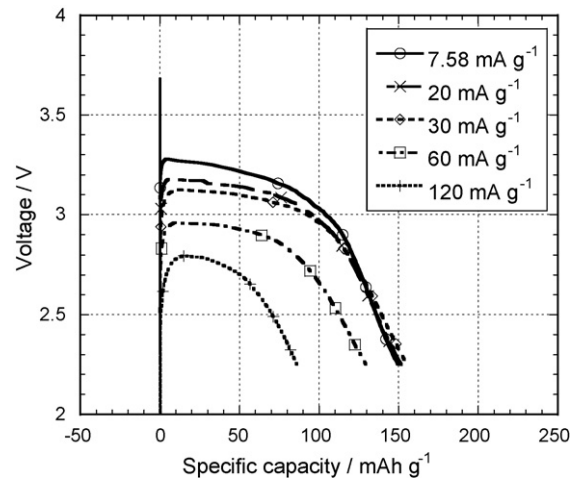**Fig. 4.** First discharge voltage profiles of SMOF perovskite at increasing current densities (7.58–120 mA g^{-1}) at room temperature.

rate capability without the use of conductive additives when discharged until 2.25 V. At relatively low currents ($\leq$30 mA g^{-1}), the specific capacity of SMOF was $\sim$150 mAh g^{-1} at a cutoff of 2.25 V. This was consistent with a theoretical 3 Li$^+$/e$^-$ reaction associated to the Ag displacement from $Ag_3MoO_3F_3$. A small decrease from 3.27 to 3.14 V in the output voltage at the 1st plateau was observed with increasing the current load from 7.58 to 30 mA g^{-1}. Increasing the current density to 60 mA g^{-1} resulted in a decrease of the specific capacity to 130 mAh g^{-1}, corresponding to 87% of the theoretical value. At a higher current load of 120 mA g^{-1}, a significant loss of the overall capacity to 86 mAh g^{-1} occurred and a relatively large degree of polarization was observed.

3.3. Electrochemical characterization

Effect of carbon black (SP): Preliminary study indicated that the rate capability of SMOF perovskite needs to be further improved. SP is a well known networked carbon black that is commonly used in the lithium battery electrodes. The effect of the carbon black on the rate capability of SMOF perovskite was investigated by
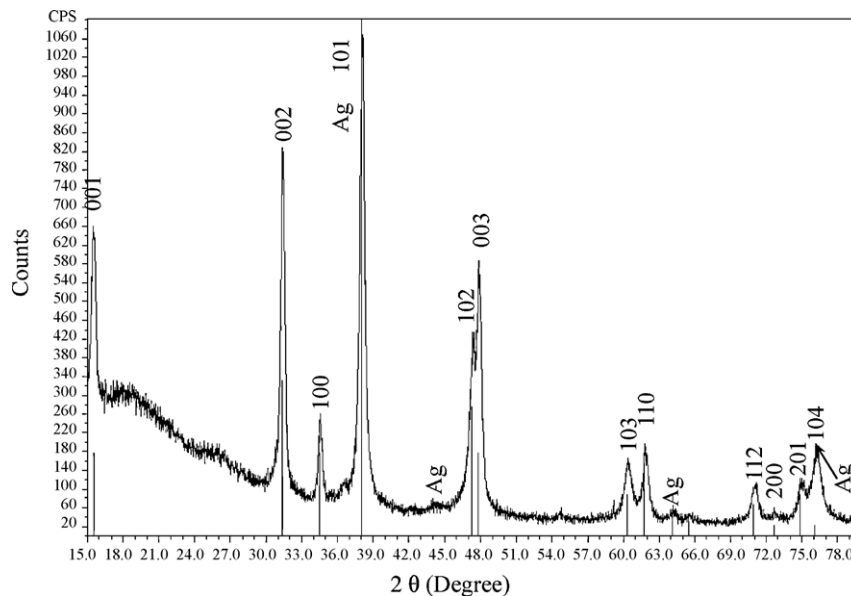
Fig. 3. Observed XRD pattern of Ag_2F showing the disparity in the relative intensity of the Bragg peaks with indexing (0 0 L). The observed Bragg diffractions of Ag_2F are denoted as ($h\,k\,l$), the vertical lines show the Bragg diffractions with referring to PDF # 00-17-0325.
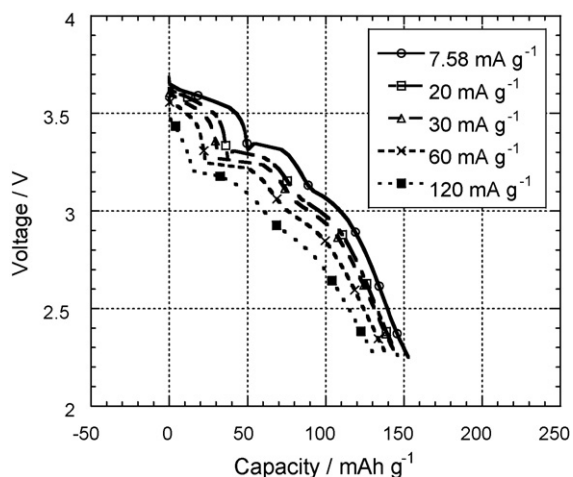
Fig. 5. First discharge voltage profiles of manually mixed 80 SMOF:20 SP (wt%) at increasing current densities (7.58–120 mA g^{-1}) at room temperature.

two different procedures: hand mixing and high-energy milling 80 SMOF:20 SP (wt%). Relative to high-energy milled SMOF and SP (not shown for figure clarity), manually mixed SMOF and SP exhibited an excellent rate capability and a much smaller degree of polarization (Fig. 5). At a relatively low current ($\leq$30 mA g^{-1}), the cells delivered a specific capacity of approximately 153 mAh g^{-1}, which was similar to pure SMOF perovskite. In contrast to pure SMOF perovskite, only a small loss in the specific capacity was observed in

the manually mixed SMOF and carbon at a high current density of 120 mA g^{-1}. The discharge profile was maintained at a relatively high potential (>3 V), and the overall specific capacity was about 132 mAh g^{-1}, which was 86% of the initial capacity obtained at the low current (7.58 mA g^{-1}).

3.4. Electrochemical characterization

Effect of metallic Ag$_2$F phase: Although to our knowledge never demonstrated, the Ag$_2$F phase is expected to be electrochemically active. The theoretical specific capacity of Ag$_2$F phase is calculated to be 114 mAh g^{-1} associated to 1 e$^-$ transfer. Indeed, this phase may contribute capacity relative to the inactive carbon black although the specific capacity of the pure Ag$_2$F shown in Fig. 6(a) is lower than that of the theoretical expectation. This difference may be a result of slow diffusion of the Li$^+$ ions within the lattice structure of Ag$_2$F. *The SMOF*: Ag$_2$F composites were fabricated through three different procedures: (1) high-energy milling (20 min) 70 SMOF:30 Ag$_2$F (wt%), (2) manual mixing 70 SMOF:30 Ag$_2$F (wt%), (3) high-energy milling (45 min) the mixtures of AgF, MoO$_3$ and Ag precursors with the intended stoichiometry of 70 SMOF to 30 Ag$_2$F (wt%). The relatively high loading of Ag$_2$F conductive additive (30 wt%) was chosen to minimize the difference between the electronic conductivity of the positive electrodes consisting of Ag$_2$F and SP as the electronic conductivity of Ag$_2$F (7.89 × 10^{-2} S cm^{-1}) is slightly lower than that of SP ($\sim$10^{-1}–10^2 S cm^{-1}) [24]. Table 2 presents the theoretical and apparent densities of the positive electrodes consisting of Ag$_2$F and SP. The apparent densities of the
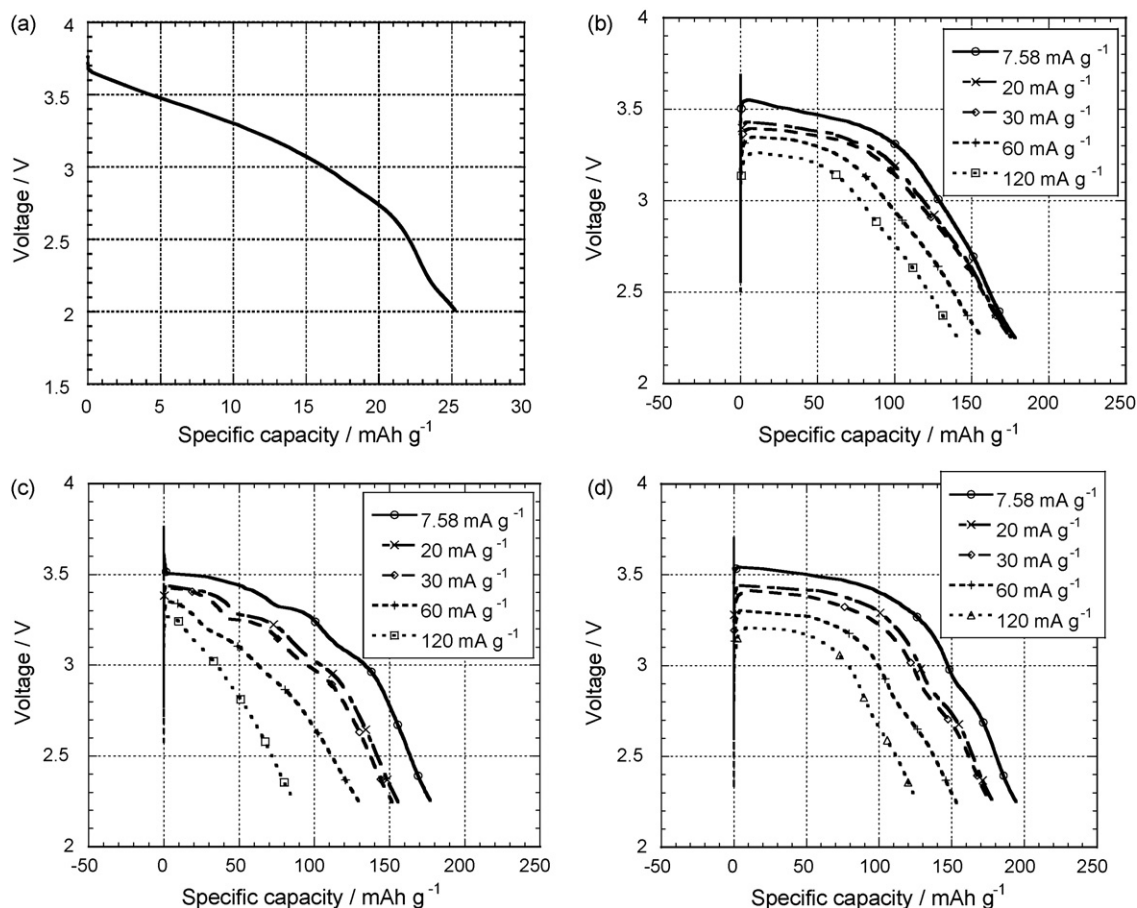

Fig. 6. First discharge voltage profiles of (a) Ag$_2$F at a current rate of 7.58 mA g^{-1}, (b) high-energy milled (20 min) 70 SMOF:30 Ag$_2$F (wt%), (c) manually mixed 70 SMOF:30 Ag$_2$F (wt%), (d) high-energy milled (45 min) the mixtures of AgF, MoO$_3$ and Ag with the intended composition of 70 SMOF:30 Ag$_2$F (wt%) at increasing current densities (7.58–120 mA g^{-1}) at room temperature.

Table 2

Density and low rate capacity of the as-fabricated SMOF composites. Label "+" indicates samples were prepared by hand mixing. Label "−" indicates samples are prepared by high-energy milling (M = min).

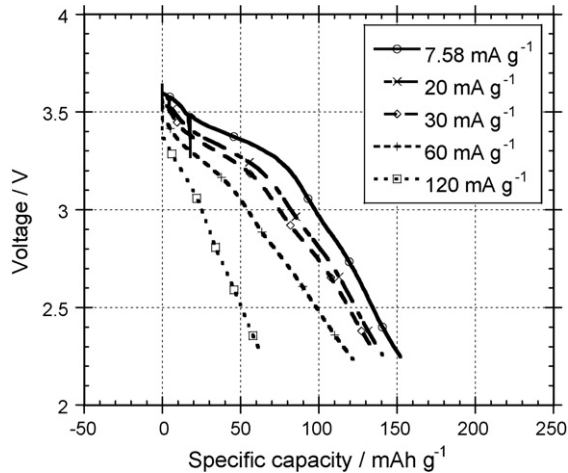| Sample	Theoretical density (g cc^{-1})	Apparent density (g cc^{-1})	Low rate capacity (mAh cc^{-1})
Ag$_2$F	8.76	7.408	
SMOF	6.224	5.832	872
80 wt% SMOF + 20 wt% SP	5.35	3.60	441
70 wt% SMOF–30 wt% Ag$_2$F – 20 M	6.985	6.804	848
70 wt% SMOF + 30 wt% Ag$_2$F	6.985	6.52	
70 wt% (AgF–MoO$_3$)–30 wt% (Ag–AgF) – 45 M	6.985	6.791	
70 wt% SMOF–30 wt% Ag – 20 M	7.507	6.515	

Fig. 7. First discharge voltage profiles of high-energy milled (20 min) 70 SMOF:30 Ag (wt%) at increasing current densities (7.58–120 mA g^{-1}) at room temperature.

composites were measured by pressing the pellets around 7000 psi. As expected, the apparent density of manually mixed SMOF + Ag$_2$F pellet is 6.52 g cc^{-1}, which is much higher than that of manually mixed SMOF + SP (3.60 g cc^{-1}).

The discharge profiles collected under various rates from cells containing high-energy milled SMOF: Ag$_2$F composites are shown in Fig. 6(b). The degree of polarization for these composites was much less than that of pure SMOF, even at a very high current load of 120 mA g^{-1} the approximate output voltage at the 1st plateau was 3.28 V. Regardless of its high density relative to manually

mixed SMOF + SP composites, these composites yielded a higher capacity of approximately 175 mAh g^{-1} at a relatively low current ($\leq$30 mA g^{-1}). Increasing the current density to 120 mA g^{-1} resulted in the retention of 140 mAh g^{-1}. Therefore, this active material is expected to deliver a much higher volumetric energy density than that of SMOF containing SP at various current rates. As shown in Table 2, at a low current (7.58 mA g^{-1}), the volumetric capacity of high-energy milled SMOF and Ag$_2$F composites is 848 mAh cc^{-1} of composites, which is 192% of the 441 mAh cc^{-1} of composites obtained by discharging manually mixed SMOF + SP composites. If a calculation is extended to lower carbon black composition (5 wt%), and we assume the rate utilization will remain the same, then the theoretical volumetric capacity is expected to be 783 mAh cc^{-1}, which is still 8% lower than that containing 30 wt% Ag$_2$F additive.

The performance of the electrodes containing manually mixed SMOF + Ag$_2$F composites is shown in Fig. 6(c). At a relatively low rate ($\leq$30 mA g^{-1}), these composites were able to deliver a similar amount of specific capacity ($\sim$150 mAh g^{-1}) to those prepared by high-energy milling SMOF: Ag$_2$F. However, a very low specific capacity (86 mAh g^{-1}) was yielded with increasing discharge rate to 120 mA g^{-1}.

Fig. 6(d) contains data from cells containing high-energy milled the mixtures of AgF, MoO$_3$ and Ag with the intended composition of 70 SMOF:30 Ag$_2$F (wt%). The cell discharged at a relatively low current ($\leq$30 mA g^{-1}) delivered a very high specific capacity of $\sim$175 mAh g^{-1}. This is comparable to that of high-energy milled SMOF and Ag$_2$F. However, at a higher discharge rate of 120 mA g^{-1}, the cell became polarized to a larger extent and the totally delivered capacity decreased to 126 mAh g^{-1}.
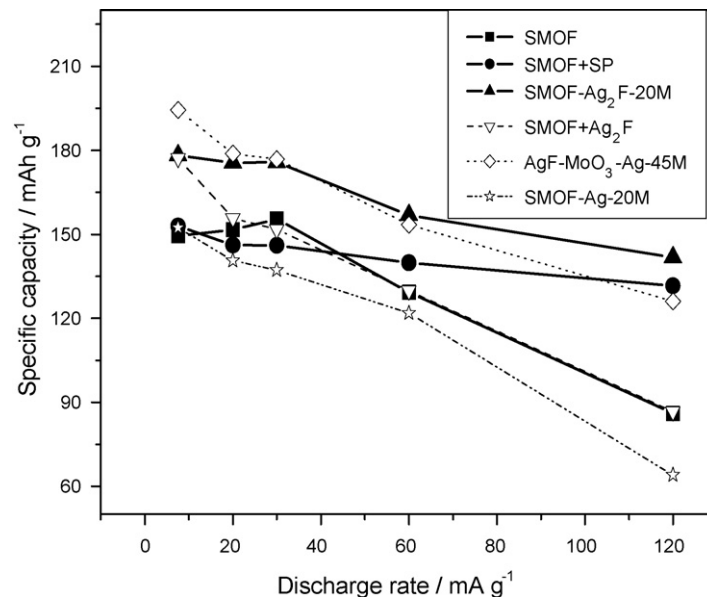

Fig. 8. Rate study data compile: specific capacity (mAh g^{-1}) as a function of discharge rate (mA g^{-1}).

3.5. Electrochemical characterization

Effect of Ag metal phase: It is apparent both in this work and our previous work that a small amount of Ag may be present in the composites. In order to compare the effect of Ag_2F vs. Ag metal phase on the rate capability of SMOF, an electrochemical study was performed on the cells containing cathode materials prepared by high-energy milling (20 min) 70 wt% SMOF and 30 wt% Ag. The voltage profiles are shown in Fig. 7. Compared to pure SMOF, a smaller degree of polarization was observed, however, it can be clearly seen that the addition of an increased amount of Ag into SMOF resulted in a poor electrochemical performance. This could be due to the disadvantageous barrier of Ag for the transport of the Li$^+$ and the fact that the distribution of Ag is far from being optimized [25].

4. Discussion

A summary of the electrochemical results is given in Fig. 8. The figure shows the capacity retention of different samples at increasing specific currents. The data clearly shown the addition of 30 wt% Ag resulted in a lower rate capability than pure SMOF electrodes, on the contrary, both carbon black (as expected) and Ag_2F played a significant role in improving the rate capability of SMOF. Relative to manually mixed SMOF + SP composites, high-energy milled SMOF and Ag_2F composites have higher rate capabilities and better low rate capacities possibly due to the electrochemical contribution of Ag_2F.

Although the milled composite of SMOF–Ag_2F has the highest rate and energy density relative to the other composites, it does not exhibit the highest initial electronic conductivity. Indeed the best sample exhibited an electronic conductivity of 5–6 orders of magnitude lower than the other samples. This suggests the advantage of the conductivity lies in the very fine distribution of the relatively high modulus (relative to silver) Ag_2F and its subsequent displacement of metallic Ag during the lithiation reaction results in a marked increase in the electronic conductivity of the composite. This proposed reaction mechanism needs to be confirmed via a suite of in situ XRD and transport measurements.

5. Conclusions

Metallic Ag_2F phase has been successfully fabricated through the use of Ag and AgF by a high-energy milling process. The electronic conductivity of Ag_2F phase was measured to be 7.89×10^{-2} S cm^{-1}. The effect of Ag_2F phase on the rate capability of SMOF perovskite was investigated. Results indicated that a higher specific capacity was delivered in the case of high-energy milled SMOF + Ag_2F electrode, suggesting Ag_2F phase can possibly be utilized as an alternative conducting agent. In terms of its very high density of AgF_2 ($\rho = 8.76$ g cc^{-1}) relative to that of SP ($\rho = 1.86$ g cc^{-1}) and its ability to electrochemically distribute highly conductive Ag during its intrinsic conversion reaction, Ag_2F is attractive as an alternative conductive agent for high volumetric energy density applications.

References

[1] R.J. Brodd, K.R. Bullock, R.A. Leising, R.L. Middaugh, J.R. Miller, E. Takeuchi, J. Electrochem. Soc. 151 (2004) K1.
[2] H. Yoshizawa, T. Ohzukub, J. Power Sources 174 (2007) 813.
[3] K. Kang, Y.S. Meng, J. Bréger, C.P. Grey, G. Ceder, Science 311 (2006) 977.
[4] T. Takeuchi, M. Tabuchi, K. Ado, K. Tatsumi, J. Power Sources 174 (2007) 1063.
[5] C.F. Holmes, J. Power Sources 97 (2001) 739.
[6] R. Latham, R. Linford, W. Schlindwein, Solid State Ionics 172 (2004) 7.
[7] F. Croce, A. D' Epifanio, J. Hassoun, A. Deptula, T. Olczac, B. Scrosatia, Electrochem. Solid-State Lett. 5 (2002) A47.
[8] H. Yamada, K. Tagawa, M. Komatsu, I. Moriguchi, T. Kudo, J. Phys. Chem. C 111 (2007) 8397.
[9] C. Wang, J. Hong, Electrochem. Solid-State Lett. 10 (2007) A65.
[10] E.S. Takeuchi, R. Leising, MRS Bull. (USA) 27 (2002) 624.
[11] E.S. Takeuchi, W.C. Thiebolt III, J. Electrochem. Soc. 135 (1988) 2691.
[12] E.M. Sorensen, H.K. Izumi, J.T. Vaughey, C.L. Stern, K.R. Poeppelmeier, J. Am. Chem. Soc. 127 (2005) 6347.
[13] F. Sauvage, V. Bodenez, H. Vezin, T.A. Albrecht, J.M. Tarascon, K.R. Poeppelmeier, Inorg. Chem. 47 (2008) 8464.
[14] W. Tong, G.G. Amatucci, ECS Trans. 11 (2008) 19.
[15] W. Tong, W.-S. Yoon, N.M. Hagh, G.G. Amatucci, Chem. Mater. 21 (2009) 2139.
[16] W. Tong, W.-S. Yoon, F. Cosandey, G.G. Amatucci, ECS Trans. 16 (2009) 107.
[17] W. Tong, G.G. Amatucci, Electrochem. Solid-State Lett. 12 (2009) A219.
[18] W. Tong, W.-S. Yoon, G.G. Amatucci, in: G. Amaratunga, A. Nathan, M. Nookala, M.C. Smart (Eds.), Mobile Energy, Mater. Res. Soc. Symp. Proc., vol. 1127E, Warrendale, PA, 2009, 1127-T03-04.
[19] N. Hamada, S. Ido, K. Kitazawa, S. Tanaka, J. Phys. C: Solid State Phys. 19 (1986) 1355.
[20] F.-J. Sun, T. Takahashi, Y. Takakuwa, H. Yaegashi, T. Sagawa, J. Phys. Soc. Jpn. 55 (1986) 461.
[21] A. Williams, J. Phys.: Condens. Matter. 1 (1989) 2569.
[22] S. Ido, S. Uchida, K. Kitazawa, S. Tanaka, J. Phys. Soc. Jpn. 57 (1988) 997.
[23] W. Tong, W.-S. Yoon, G.G. Amatucci, J. Power Sources 195 (2010) 6831.
[24] R.W.A. Franco, J.P. Donoso, C.J. Magon, C.B. Rodella, A.O. Florentino, M.J. Saeki, J.M. Pernaut, A.L. de Oliveira, Solid State Ionics 113–115 (1998) 149.
[25] W.-J. Zhou, B.-L. He, H.-L. Li, Mater. Res. Bull. 43 (2008) 2285.